Currents Induced in the Human Body for Exposure to Ultrawideband Electromagnetic Pulses

O. P. Gandhi and Cynthia M. Furse

Abstract— The frequency-dependent finite-difference time-domain [(FD)²TD] method is used to calculate internal electric fields and induced current densities in a 1.31-cm resolution anatomically-based model of the human body for exposure to ultrawideband vertically polarized electromagnetic pulses (EMP's). From a single (FD)²TD simulation, two ultrawideband pulses with frequencies up to 1500 MHz are examined using a convolution technique. The complex permittivities $\varepsilon^*(\tau)$ for the various tissues are known to vary a great deal over the wide bandwidth of these two pulses. In the (FD)²TD formulation, these frequency-dependent $\varepsilon^*(\tau)$ are described by the best-fit second-order Debye equations for the sixteen tissues that are used to define the anatomically-based model. The vertical currents passing through several sections of the body are compared for a shoe-wearing model standing on a perfectly conducting ground plane, and a barefoot model suspended in air. For the first pulse, currents on the order of 1 to 4 mA per V/m of incident fields are calculated with the highest values calculated for the sections through the bladder and slightly above it. For the second pulse, currents on the order of 4 mA per V/m of incident fields were calculated.

I. INTRODUCTION

The anatomically-based model of the human body has previously been used to calculate induced currents for exposure to vertically-polarized electromagnetic pulses (EMP's) [1]. These EMP's had risetimes on the order of 10–30 ns, durations on the order of 100–300 ns, and bandwidths of 0–100 MHz, so the conventional nondispersive finite-difference time-domain (FDTD) method was used. In this method the tissue properties were assumed to be independent of frequency and were taken at a central frequency of 40 MHz. While the conventional FDTD method which ignores the dispersion of

the tissues' dielectric properties may be appropriate for narrowband irradiation, it is clearly not suitable for wideband irradiation such as that due to short pulses with subnanosecond risetimes and pulse durations on the order of a few nanoseconds. The FDTD algorithm was consequently modified to incorporate the frequency dispersion of the dielectric properties for the various tissues [2], [3]. Using a second-order Debye equation to model the frequency dispersion of the complex permittivity, $\varepsilon^*(\omega)$, the relation between **E** and **D** was solved in the time domain along with Faraday's and Ampere's laws to give the frequency-dependent FDTD [(FD)²TD] method. Using this method, this paper gives currents and specific absorptions (SA's) induced in the human body for exposure to two ultrawideband electromagnetic pulses with instantaneous bandwidths up to 1500 MHz.

II. THE FREQUENCY-DEPENDENT FINITE-DIFFERENCE TIME-DOMAIN ((FD)²TD) METHOD

The time-dependent Maxwell's curl equations used for the FDTD method are

$$\nabla \times \mathbf{E} = -\frac{\partial \mathbf{B}}{\partial t} = -\mu \frac{\partial \mathbf{H}}{\partial t} \tag{1}$$

$$\nabla \times \mathbf{H} = \frac{\partial \mathbf{D}}{\partial t} \tag{2}$$

where the flux density vector **D** is related to the electric field **E** through the complex permittivity $\varepsilon^*(\tau)$ of the local tissue by the following

$$\mathbf{D}(\omega) = \varepsilon^*(\omega)\mathbf{E}(\omega). \tag{3}$$

For the conventional FDTD method the complex permittivity $\varepsilon^*(\omega)$ is assumed to be independent of the frequency ω. Then (3) is substituted into (2), and (1) and (2) are solved iteratively in the time domain.

For the (F)²TD method $\varepsilon^*(\omega)$ is dependent on the frequency ω, and (3) must be converted to a form which can be solved iteratively in the time domain along with (1) and (2). This conversion may be done by choosing a rational function for $\varepsilon^*(\omega)$ such as the second-order Debye equation [2]

$$\varepsilon^*(\omega) = \varepsilon_0 \left[\varepsilon_\infty + \frac{\varepsilon_{s1} - \varepsilon_\infty}{1 + j\omega\tau_1} + \frac{\varepsilon_{s2} - \varepsilon_\infty}{1 + j\omega\tau_2} \right]. \tag{4}$$

Rearranging (4) and substituting in (3) gives

$$\mathbf{D}(\omega) = \varepsilon^*(\omega)\mathbf{E}(\omega)$$
$$= \varepsilon_0 \left[\frac{\varepsilon_s + j\omega(\varepsilon_{s1}\tau_2 + \varepsilon_{s2}\tau_1) - \omega^2\tau_1\tau_2\varepsilon_\infty}{1 + j\omega(\tau_1 + \tau_2) - \omega^2\tau_1\tau_2} \right] \mathbf{E}(\omega) \tag{5}$$

where the zero (static) frequency dielectric constant is given by

$$\varepsilon_s = \varepsilon_{s1} + \varepsilon_{s2} - \varepsilon_\infty. \tag{6}$$

Given $e^{j\omega t}$ time dependence, we can write (5) as a differential equation in the time domain

$$\tau_1\tau_2 \frac{\partial^2 \mathbf{D}}{\partial t^2} + (\tau_1 + \tau_2)\frac{\partial \mathbf{D}}{\partial t} + \mathbf{D} = \varepsilon_0 \left[\varepsilon_s \mathbf{E} + (\varepsilon_{s1}\tau_2 + \varepsilon_{s2}\tau_1)\frac{\partial \mathbf{E}}{\partial t} \right.$$
$$\left. + \varepsilon_\infty \tau_1\tau_2 \frac{\partial^2 \mathbf{E}}{\partial t^2} \right]. \tag{7}$$

For the (FD)²TD method, (1) and (2) are solved subject to (7). Similar to [1]–[4] the space and time derivatives in these equations are approximated by divided-differences, and these equations are solved
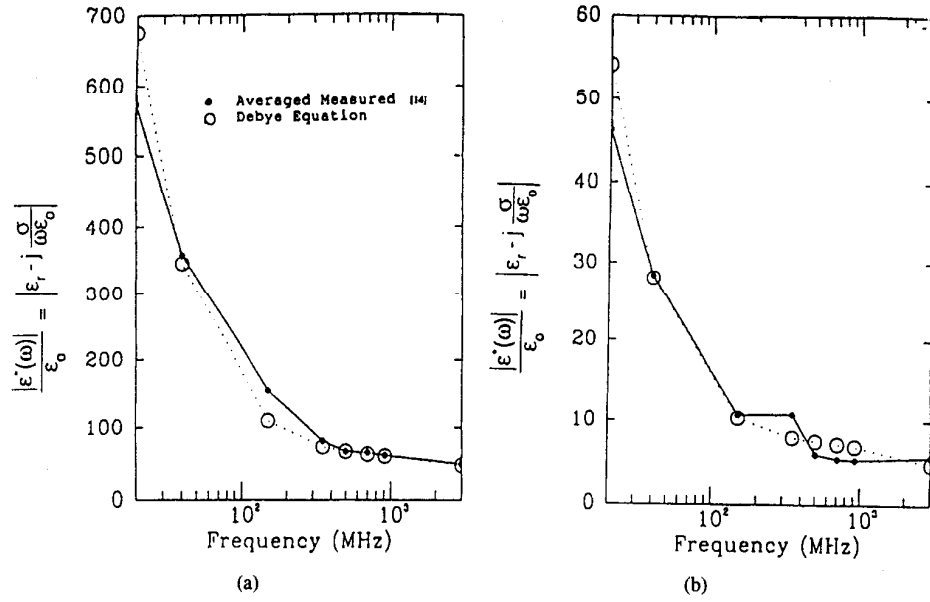
Fig. 1. Fit of second-order Debye equation (4) to measured tissue properties of: (a) muscle and (b) fat.

for E-H-D iteratively. The detailed derivation of these equations is given in [2].

A similar derivation using a first-order Debye equation is given in [5], using a second-order Lorentz equation is given in [6], using a second-order Debye equation for homogenous tissues is given in [7], and using a second-order Debye equation for heterogeneous tissues is given in [3]. A different derivation but similar application of this approach is given in [8].

Another approach to frequency dependent FDTD calculations is to convert the complex permittivity from the frequency domain and convolve this with the time-domain electric fields to obtain time-domain fields for the dispersive materials. For some rational forms of complex permittivity, this discrete convolution can be updated recursively. This approach has been applied to materials described by a first-order Debye equation in [9]–[11], a second-order Lorentz equation in [12], and a gaseous plasma in [13].

III. MODELING OF BIOLOGICAL TISSUE PROPERTIES USING THE DEBYE EQUATION

The measured properties of biological tissues (muscle, fat, bone, blood, intestine, cartilage, lung, kidney, pancreas, spleen, liver, heart, brain/nerve, skin, and eye) were obtained from [14]. Optimal values for ε_{s1}, ε_{s2}, ε_∞, τ_1 and τ_2 in (4) were obtained by nonlinear least-squares matching to the measured relative permittivity and conductivity for fat and muscle. All of the other tissue properties fall roughly between these two. The values of these two sets of optimal relaxation constants were averaged to obtain optimal average values of τ_1 and τ_2. This was done to facilitate volume-averaging of the tissue properties in cells of the heterogeneous man model. Using these averaged relaxation constants, optimal values for ε_{s1}, ε_{s2}, and ε_∞ were again found using least-squares matching and are given in Table I [3]. The comparison between the measured tissue properties and those computed from the Debye equation are shown in Fig. 1 for fat and muscle. This figure shows the magnitude of the dielectric constant, for simplicity in evaluating the broad-band fit, and the fit of the particular values of relative permittivity and conductivity is equally good. Similar comparisons were also obtained for the other tissue types.

TABLE I
DEBYE CONSTANTS FOR TISSUES $\tau_1 = 46.25$ ns AND $\tau_2 = 0.0907$ ns (AVERAGE OF OPTIMUM FOR FAT AND MUSCLE)

Tissue	ε_∞	ε_{s1}	ε_{s2}
Muscle	40.0	3948.	59.09
Bone/Cartilage	3.4	312.8	7.11
Blood	35.0	3563.	66.43
Intestine	39.0	4724.	66.09
Liver	36.3	2864.	57.12
Kidney	35.0	3332.	67.21
Pancreas/Spleen	10.0	3793.	73.91
Lung	10.0	1224.	13.06
Heart	38.5	4309.	54.58
Brain/Nerve	32.5	2064.	56.86
Skin	23.0	3399.	55.59
Eye	40.0	2191.	56.99

The 1.31-cm resolution anatomically-based man model has previously been described in [1]. This man model has been used for studies up to 915 MHz. Although the cell size at this frequency is about $\lambda_c/5.5$ in muscle, this model appears to give sufficiently good results at this frequency. This is probably because the high absorption of the tissues ameliorates the dispersion errors caused by having a cell size larger than $\lambda/10$ commonly used in FDTD simulations. Muscle is the tissue with the smallest wavelength, so other tissues are better modeled.

IV. INDUCED CURRENT CALCULATIONS

The total current distribution in layer k may be calculated one of two ways. The first is

$$I_{z,k}(t) = \delta^2 \sum_{i,j} \frac{\partial \mathbf{D}_z(i,j,k)}{\partial t} \tag{8}$$

where δ is the FDTD cell size ($\delta = 1.31$ cm), and the summations are carried out for all cells in a given layer. This method calculates the current which would be measured by a loop-type current meter around the layer. With a broadband incident pulse, parts of the layer may have positive-directed currents, while other parts simultaneously may have negative-directed currents. These currents may cancel each

other out in the summation of (8), giving the impression that the total current is relatively low.

The second total current distribution calculation is given by

$$I_{z,k}(t) = \delta^2 \sum_{i,j} \left| \frac{\partial \mathbf{D}_z(i,j,k)}{\partial t} \right|. \tag{9}$$

This gives a better measure of the total current passing through the layer and will give values greater than or equal to (8). Calculations involving $\partial D/\partial t$ were used instead of H for calculation efficiency.

V. THE CONVOLUTION METHOD

The convolution method [15] was used to allow calculation of the response of the body to several different waveforms using a single FDTD or (FD)²TD simulation with an impulse excitation. The band-limited impulse response is stored and convolved with the frequency spectrum of the waveform of interest to give the response of the body to that particular waveform.

The impulse response of several layers of the body was found for both of the current calculations given in (8) and (9). Two (FD)²TD simulations were made, one with the man model wearing shoes and standing on a perfectly conducting ground plane, and the other with the man model suspended in air (the isolated model). The shoe-wearing condition was modeled by a 2.62-cm (2δ) thickness of rubber ($\varepsilon_r = 4.0$) between the foot and the ground plane. The frontally-incident plane-wave was vertically-polarized. For a cell size of $\delta_x = \delta_y = \delta_z = \delta = 1.31$ cm, the time step was $\delta_\tau = \delta/2c_o = 21.83$ ps. A rectangular pulse 6 time steps $= 6\,\delta_\tau = 131$ ps in duration was used as the impulse incident waveform. The currents induced in each layer by a waveform of interest, $\mathbf{E}^{des}$, are then found from

$$I^{des}(t) = \mathcal{F}^{-1}\left\{ \frac{\mathcal{F}\{E^{des}(t)\}\mathcal{F}\{I^{imp}(t)\}}{\mathcal{F}\{E^{imp}(t)\}} \right\} \tag{10}$$

where

$E^{des}(t)$ desired time domain incident waveform;

$E^{imp}(t)$ impulse time domain incident waveform (rectangular pulse of width $6\delta t = 131$ ps);

$I^{imp}(t)$ impulse response current;

$I^{des}(t)$ desired response current;

$\mathcal{F}$ Fourier transform.

As in [15], a rectangular pulse was chosen for convenience. Any other pulse with significant frequency components covering the entire band of the desired incident waveform could be used. Equation (10) does not result in a divide by zero when using the rectangular pulse, because in the band of interest, the spectrum of the rectangular pulse is almost exactly 1.0.

The convolution method was validated by comparing the results obtained running the (FD)²TD method with the rectangular pulse, and convolving the time-domain output with the desired waveform to the results obtained running the (FD)²TD method directly with the desired waveform. The results were virtually indistinguishable. The use of the convolution method is only efficient if two or more waveforms are to be analyzed.

VI. COUPLING OF AN ULTRAWIDEBAND PULSE TO THE HUMAN BODY

The first ultrawideband pulse, prescribed for the time domain $0 \le t \le 10$ ns, is shown in Fig. 2(a). This pulse has a rise time of about 0.2 ns and a total time duration of about 7–8 ns. The frequency spectrum of this pulse is shown in Fig. 2(b). Most of the energy in the pulse is concentrated in the 200–900 MHz band with the peak of the energy about 500 MHz. The incident field was taken to be vertically polarized, since this polarization is known to result in the strongest coupling for standing individuals. The temporal variations of the
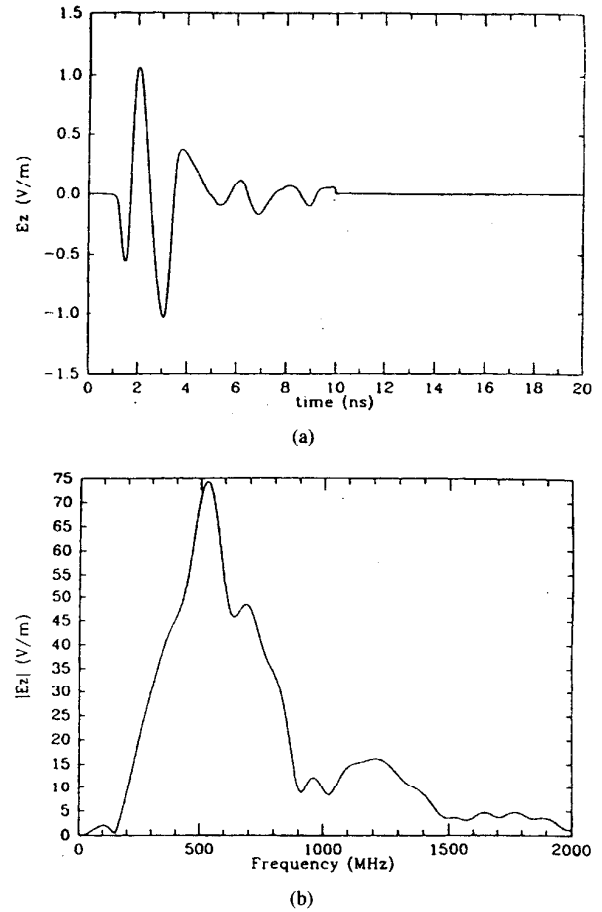

Fig. 2. (a) The first prescribed electromagnetic pulse of peak incident field = 1.1 V/m and (b) its frequency spectrum.

layer-averaged vertical currents for the various sections of the body were calculated for both grounded shoe-wearing and ungrounded barefoot exposure conditions of the model. The current variations calculated using (8) for some representative sections such as those through the eyes, heart, and bladder are shown in Fig. 3(a)–(c), respectively.

The peak time-domain current for each layer of the body is shown in Fig. 4 for the current calculations using (8). The maximum peak current of 3.5 mA, which is 3.2 mA per V/m occurs at a height of 96.3 cm (38 in.) above the bottom of the feet. A very similar result had previously been observed for calculations using isolated and grounded models of the human body for plane-wave exposures at frequencies of 350–700 MHz where the highest induced currents on the order of 3.0–3.2 mA per V/m were calculated for sections of the body that are at heights of 85–100 cm above the feet [16], [17].

The frequency spectra of the currents shown in Fig. 3(a)–(c) for the various sections of the body are shown in Fig. 5(a)–(c). As expected, components from low frequencies to frequencies in excess of 1000 MHz are observed. From Fig. 5(a)–(c) it is obvious that any instrumentation to measure the induced currents through the feet or at any location of the body must have a bandwidth in excess of 1000 MHz and subnanosecond response time.

The currents analyzed thus far have been calculated using (8), which represents the total currents which would be measured using a loop-type current meter around a layer of the body. For these ultrawideband pulses, however, the positive and negative currents which are simultaneously present in the body as seen in Fig. 3 will
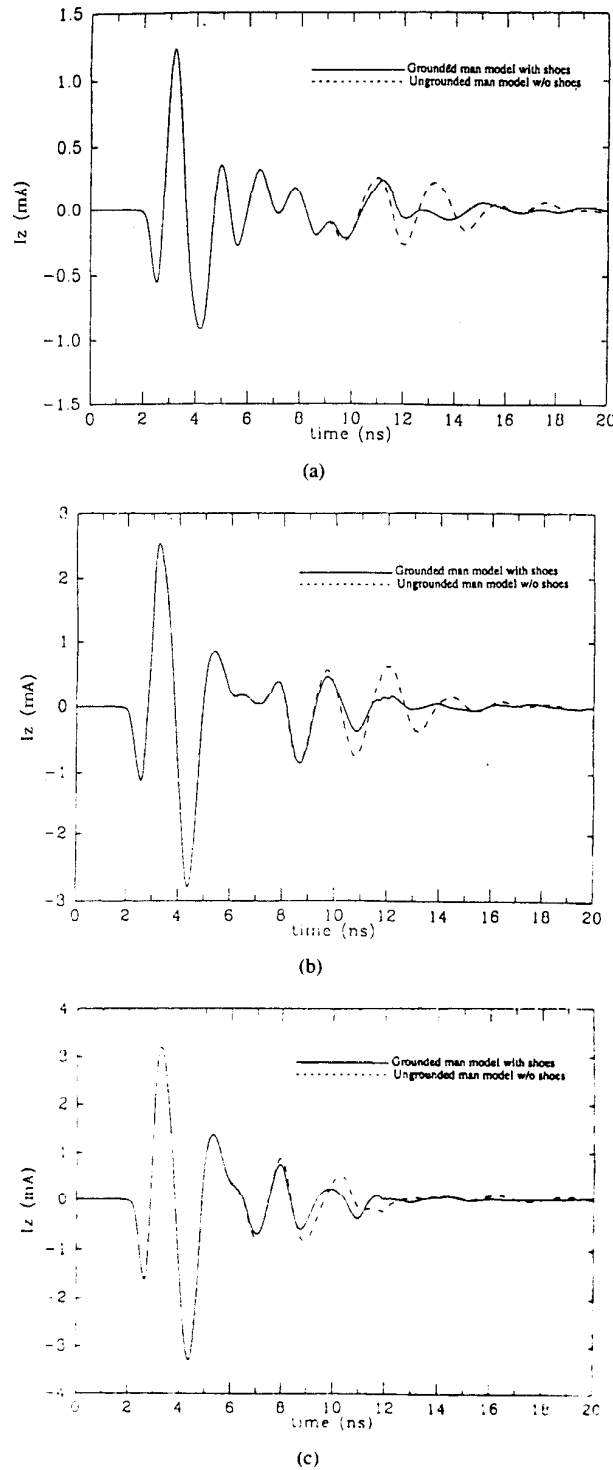
(a)

(b)

(c)

Fig. 3. Currents induced for the various sections of the body calculated using (8) for the incident pulse of Fig. 2: (a) section through the eyes (168.3 cm above bottom of feet), (b) section through the heart (135.6 cm above bottom of feet), and (c) section through the bladder (91.0 cm above bottom of feet).

often at least partially cancel each other out, so the current summation given in (9) actually gives a better measure of the magnitude of the current passing through each layer. Using the calculation in (9), the currents were again calculated for the grounded shoe-wearing man model and for the isolated model, and the temporal variations
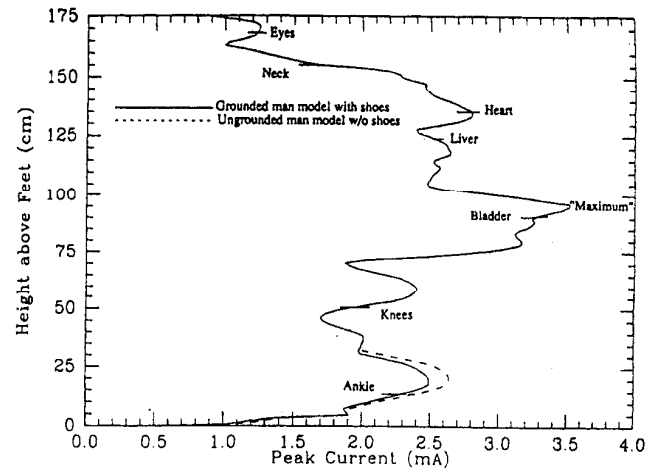

Fig. 4. Peak currents induced in the various sections of the body for grounded shoe-wearing and ungrounded barefoot (isolated) conditions of the model. Incident field is the EMP of Fig. 2. Currents are calculated using (8).

of the currents are shown in Fig. 6(a)–(c) for the sections through the eyes, heart, and bladder, respectively. The peak current passing through each layer is shown in Fig. 7, and, as expected, the values are significantly higher than those shown in Fig. 4.

A second ultrawideband pulse is shown in Fig. 8(a). Its frequency spectrum is shown in Fig. 8(b) and is found to extend from zero to over 1000 MHz. Using the convolution method, the currents are found from the same $(FD)^2TD$ simulation that was used to obtain results for the first EMP. The peak currents calculated using (8) in each layer are shown in Fig. 9. Peak values on the order of 5 mA per V/m are obtained, which are similar to the values shown in Figs. 4 and 7 for the ultrawideband pulse of Fig. 2. Calculating the layer-averaged currents using (8) or (9) did not significantly change the results for this pulse, as simultaneous positive and negative currents were not generally observed in a single layer. This is perhaps partly because the pulse itself has very little negative component.

VII. SPECIFIC ABSORPTION CALCULATIONS

The layer-averaged specific absorption for layer k is given by

$$SA_{layer\,k} = \frac{\delta t}{N_k} \sum_t \sum_{i,j} \frac{E(i,j,k,t)}{\rho(i,j,k)} \cdot \frac{\partial D(i,j,k,t)}{\partial t} \quad (11)$$

where δt is the time step ($\delta t = 21.83$ ps) used for time-domain calculations, N_k is the number of cells in the kth layer of the body, and $\rho(i,j,k)$ is the mass density in kg/m^3 for each of the cells in the corresponding layers. The layer-averaged specific absorption for the EMP in Fig. 2(a) is shown in Fig. 10 as a function of height above the feet for both the grounded, shoe-wearing model and the isolated model. Note that because of the very limited time duration of the pulse (7–8 ns) the specific absorptions are on the order of 0.02 to 0.20 pJ/kg.

VIII. TOTAL ENERGY CALCULATION

The total energy, W, absorbed in the body is calculated from

$$W = \delta t \delta^3 \sum_t \sum_{i,j} E(i,j,k,t) \cdot \frac{\partial D(i,j,k,t)}{\partial t}. \quad (12)$$

For the model exposed to the first ultrawideband pulse shown in Fig. 2, the energy is virtually all absorbed in the first 6 to 8 ns. The total energy absorbed by the body exposed to a single pulse is
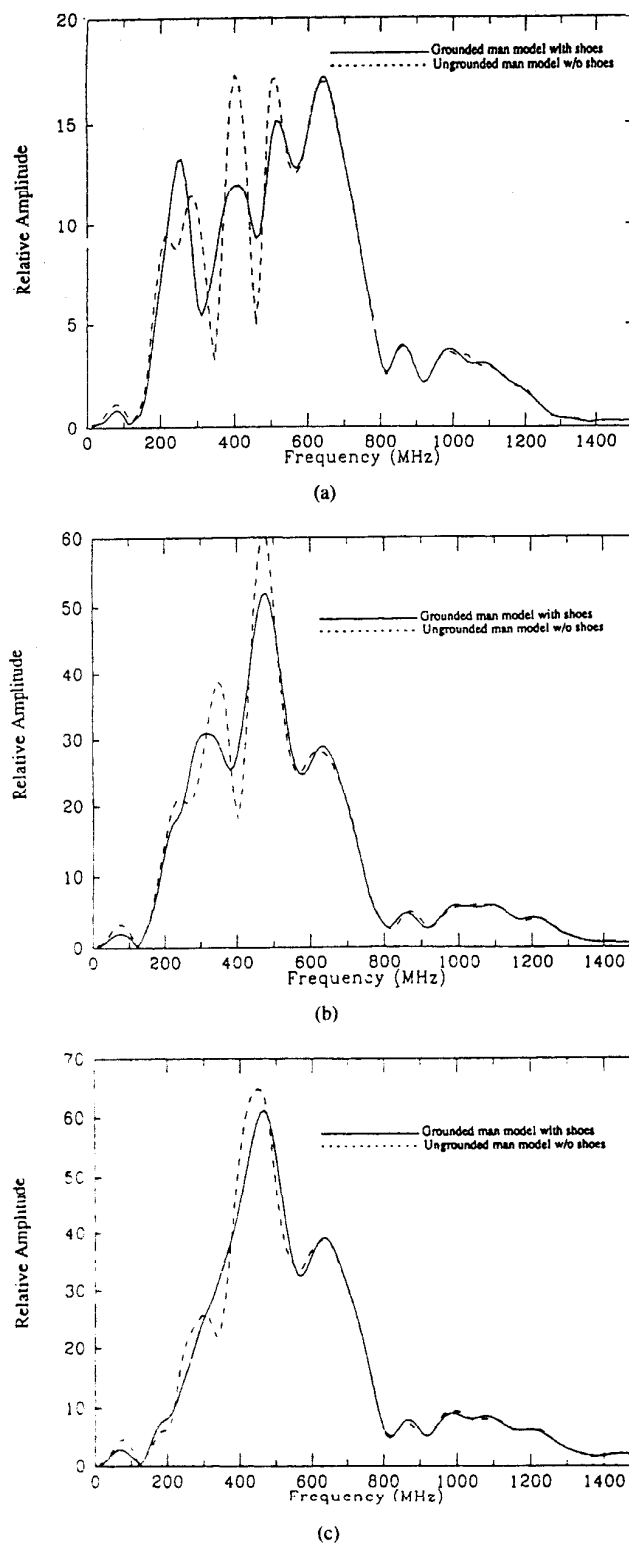
(a)

(b)

(c)

(a)

(b)

(c)

Fig. 5. Frequency spectra of the currents shown in Fig. 4. Incident field is the ultrawideband EMP of Fig. 2. Currents are calculated using (8): (a) section through the eyes (168.3 cm above bottom of feet), (b) section through the heart (135.6 cm above bottom of feet), and (c) section through the bladder (91.0 cm above bottom of feet).
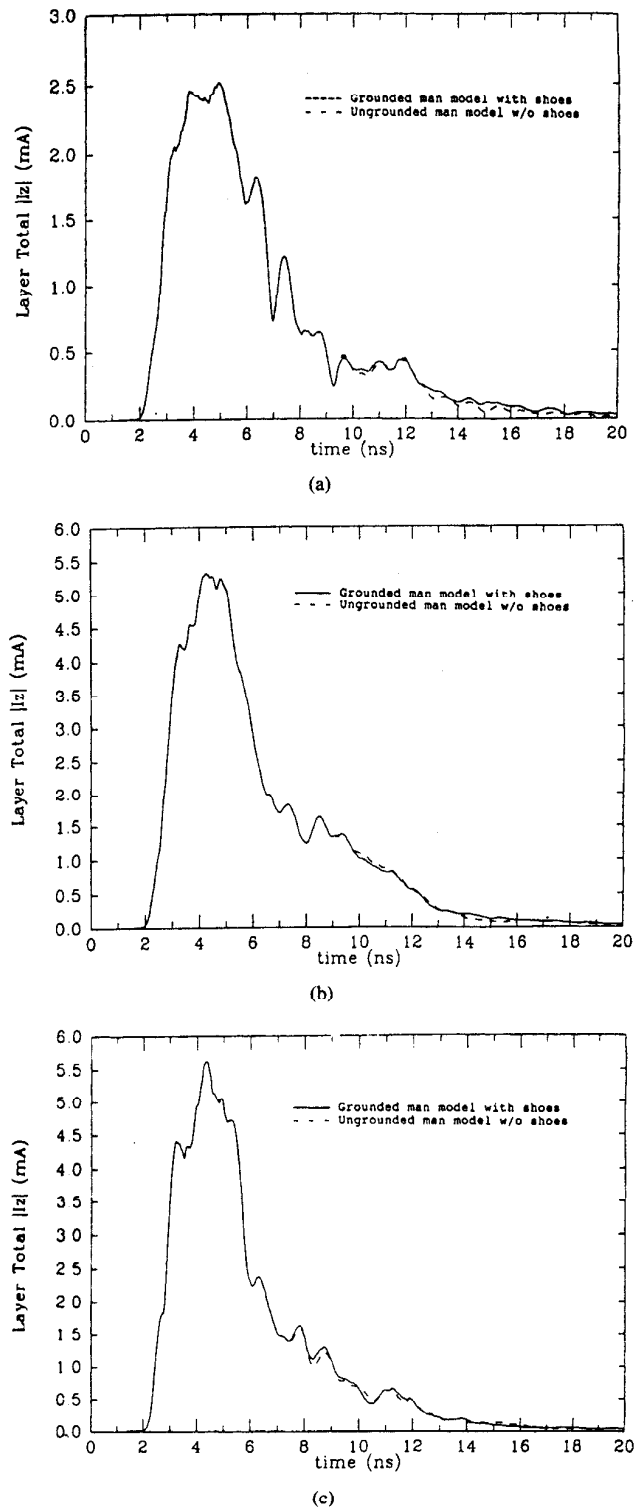
Fig. 6. Currents induced for the various sections of the body calculated using (9) for the incident pulse of Fig. 2: (a) section through the eyes (168.3 cm above bottom of feet), (b) section through the heart (135.6 cm above bottom of feet), and (c) section through the bladder (91.0 cm above bottom of feet).

calculated to be 2.0 and 1.91 pJ for isolated and grounded, shoe-wearing conditions, respectively.

IX. PROJECTIONS FOR HIGHER PULSE AMPLITUDES AND REPETITION RATES

In the event the body is irradiated by a train of pulses, it is recognized that the SA and absorbed energy should be multiplied
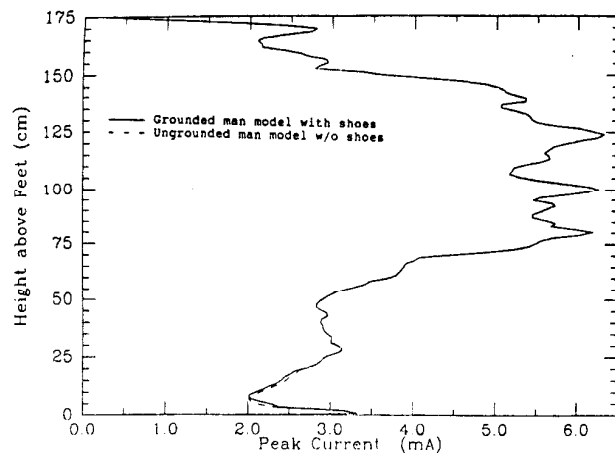
Fig. 7. Peak currents induced in the various sections of the body for grounded shoe-wearing and ungrounded barefoot (isolated) conditions of the model. Incident field is the EMP of Fig. 2. Currents are calculated using (9).
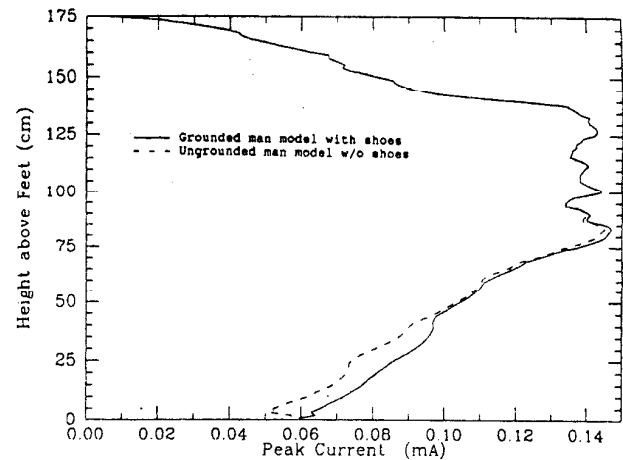

Fig. 9. Peak currents induced in the various sections of the body for grounded shoe-wearing and ungrounded barefoot (isolated) conditions of the model. Incident field is the EMP of Fig. 8. Currents are calculated using (8).
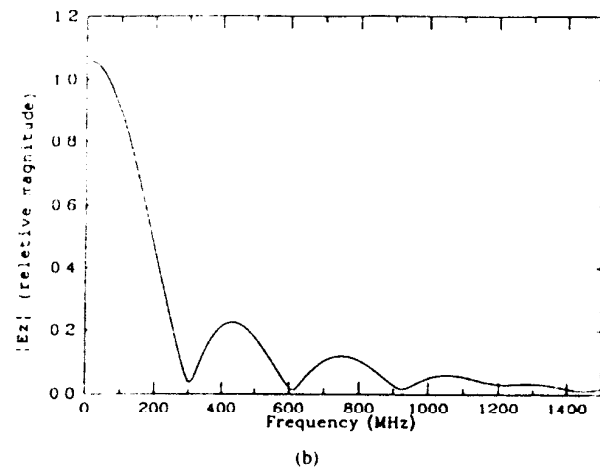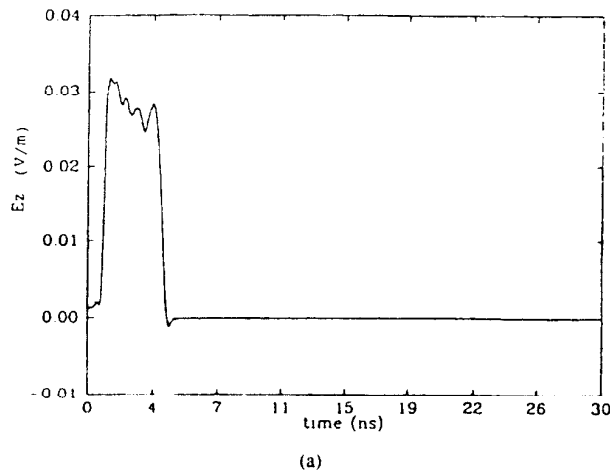

(a)

(b)

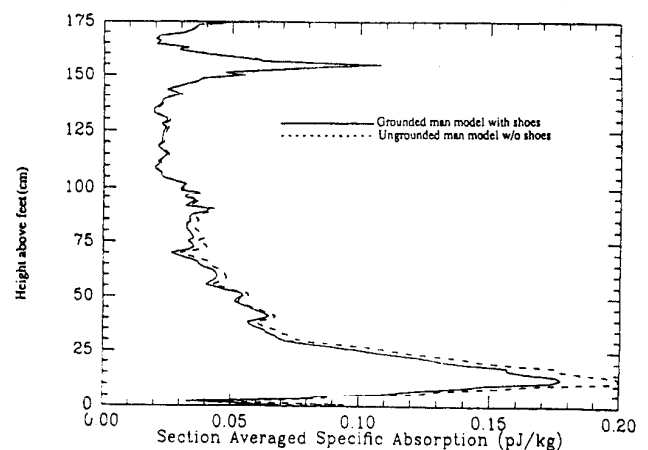Fig. 8. (a) The second prescribed electromagnetic pulse and (b) its frequency spectrum.

Fig. 10. Variation of section or layer-averaged specific absorption for the ultrawideband pulse of Fig. 2. $E_{peak} = 1.1$ V/m.

by the square of the peak incident field amplitude and the pulse repetition rate.

To illustrate, suppose that the pulse peak amplitude is 1 kV/m rather than 1.1 V/m that has been assumed for the ultrawideband pulse of Fig. 2. Furthermore, suppose that the pulse repetition rate is 1000 pulses per s rather than a single pulse. For such a train of pulses for any 6 min period there would be 3.6×10^5 pulses. Peak specific absorption for the various sections of the body (from Fig. 9) would be on the order of $(0.18 \text{ pJ/kg})(10^3 V/m/1.1 \text{ V/m})^2 (3.6 \times 10^5 \text{ pulses}) = 53.5$ mJ/kg. Similarly the total energy absorbed by the body in any 6-min period would be 0.59 and 0.57 J for isolated and grounded, shoe-wearing conditions, respectively. Both the SA's and the whole-body absorption are considerably less than the 6-min averaged values of 144 J/kg and 10 080 J, respectively, that are suggested in the ANSI/IEEE C95.1-1992 RF safety guidelines [18].

For a 1 kV/m peak amplitude pulse the induced peak currents for the various layers of the body can be similarly scaled from the values given in Figs. 4 and 7 for a 1.1 V/m peak amplitude pulse shown in Fig. 2. Induced peak currents on the order of 1.1–3.2 A are calculated for a 1 kV/m peak amplitude pulse, and the values would be proportionally higher for larger amplitude pulses.

X. CONCLUSION

Using the $(FD)^2TD$ and convolution methods, this paper describes the currents induced in a 1.31-cm resolution anatomically-based mod-

els of the human body for exposure to ultrawideband electromagnetic pulses. Specific absorptions and total energy absorbed in the body are also calculated. Using a scaling factor to examine higher-amplitude pulse trains, the SA's and whole-body absorption were found to be well within the ANSI-IEEE safety guideline for the two pulses examined.

REFERENCES

[1] J.-Y. Chen and O. P. Gandhi, "Currents induced in an anatomically based model of a human for exposure to vertically polarized electromagnetic pulses," *IEEE Trans. Microwave Theory Tech.*, vol. 39, pp. 31–39, 1991.

[2] O. P. Gandhi, B.-Q. Gao, and J.-Y. Chen, "A frequency dependent finite difference time domain formulation for general dispersive media," *IEEE Trans. Microwave Theory Tech.*, vol. 41, pp. 658–665, 1993.

[3] C. M. Furse, J.-Y. Chen, and O. P. Gandhi, "Use of the frequency-dependent finite difference time domain method for induced current and SAR calculations for a heterogeneous model of the human body," *IEEE Trans. Electromag. Compat.*, pp. 128–133, May 1994.

[4] A. Taflove and K. R. Umashankar, "The finite-difference time-domain method for numerical modeling of electromagnetic wave interactions with arbitrary structures," in *Progress in Electromagnetic Research 2*, M. A. Morgan Ed. New York: Elsevier, 1990, ch. 8, pp. 287–373.

[5] R. M. Joseph, S. C. Hagness, and A. Taflove, "Direct time integration of Maxwell's equations in linear dispersive media with absorption for scattering and propagation of femtosecond electromagnetic pulses," *Opt. Lett.*, vol. 16, no. 18, pp. 1412–1414, 1991.

[6] C. F. Lee, R. T. Shin, and J. A. Kong, "Application of FD-TD technique to dispersive materials," in *PIERS Proc.*, 1991.

[7] O. P. Gandhi, B.-Q. Gao, and J.-Y. Chen, "A frequency-dependent finite-difference time-domain formulation for general dispersive media," *IEEE Trans. Microwave Theory Tech.*, vol. 41, pp. 658–665, 1993.

[8] D. M. Sullivan, "Frequency-dependent FDTD methods using Z transforms," *IEEE Trans. Antennas Propagat.*, vol. 40, pp. 1223–1230, 1992.

[9] R. J. Luebbers, F. P. Hunsberger, K. S. Kunz, R. B. Standler, and M. Schneider, "A frequency-dependent finite-difference time-domain formulation for dispersive materials," *IEEE Trans. Electromag. Compat.*, vol. 32, pp. 222–227, 1990.

[10] M. D. Bui, S. S. Stuchly, and G. I. Costache, "Propagation of transients in dispersive media," *IEEE Trans. Microwave Theory Tech.*, vol. 40, pp. 532–539, 1992.

[11] D. M. Sullivan, "A frequency-dependent FDTD method for biological applications," *IEEE Trans. Microwave Theory Tech.*, vol. 40, pp. 532–539, 1992.

[12] R. J. Luebbers and F. Hunsberger, "FDTD for Nth order dispersive media," *IEEE Trans. Antennas Propagat.*, vol. 40, pp. 1297–1301, 1992.

[13] R. J. Luebbers, F. Hunsberger, and K. S. Kunz, "A frequency-dependent finite-difference time-domain formulation for transient propagation in plasma," *IEEE Trans. Antennas Propagat.*, vol. 39, pp. 29–34, 1991.

[14] C. H. Durney *et al.*, "Radiofrequency radiation dosimetry handbook," 4th ed, USAF School of Aerospace Medicine, Brooks AFB, TX, Rep USAF SAM-TR-85-73, 1986.

[15] J.-Y. Chen, C. M. Furse, and O. P. Gandhi, "A simple convolution procedure for calculating currents induced in the human body for exposure to electromagnetic pulses," *IEEE Trans. Microwave Theory Tech.*, vol. 42, pp. 1172–1175, July 1994.

[16] O. P. Gandhi, Y.-G. Gu, J.-Y. Chen, and H. I. Bassen, "Specific absorption rate and induced current distributions in an anatomically based human model for plane-wave exposures," *Health Physics*, vol. 63, no. 3, pp. 281–290, 1992.

[17] O. P. Gandhi, Y.-G. Gu, and J.-Y. Chen, "SAR and induced current distributions in anatomically based models of a human for plane-wave exposures at frequencies 20–915 MHz," Depart. Microwave Research, Walter Reed Army Institute of Research, Washington, DC, Final Rep. Contract DAMD 17-90-M-SA 49, Aug. 27, 1990.

[18] IEEE Standard for Safety Levels with Respect to Human Exposure to Radiofrequency Electromagnetic Fields, 3 kHz to 300 GHz, ANSI/IEEE Standard C95.1-1992, 1992.